Out-of-plane magnetic domain structure in a thin film of $La_{0.67}Sr_{0.33}MnO_3$ on $SrTiO_3$ (001) observed by magnetic force microscopy

E. P. Houwman,[1,*] G. Maris,[2] G. M. De Luca,[1,†] N. Niermann,[2] G. Rijnders,[1] D. H. A. Blank,[1] and S. Speller[2]
[1]MESA+-*Institute of Nanotechnology, University of Twente, P.O. Box 217, 7500 AE Enschede, The Netherlands*
[2]*Institute for Molecules and Materials, Radboud University, Toernooiveld 1, 6525 ED Nijmegen, The Netherlands*
(Received 29 October 2007; revised manuscript received 18 March 2008; published 13 May 2008)

The room temperature out-of-plane magnetization of epitaxial thin films of $La_{0.67}Sr_{0.33}MnO_3$ on $SrTiO_3$ (001) has been investigated with magnetic force microscopy, using magnetic tips with very small coercivity, relative to the film. A clear magnetic pattern in the form of a checkerboard, with domain dimensions of a few hundred nanometers, was found for the thin, coherently strained films, which is approximately aligned along the maximum strain [110] and $[1\bar{1}0]$ directions in the film. With increasing in-plane applied magnetic field, the magnetic contrast reduces, reflecting the rotation of the magnetization vector into the plane of the film. This process is reversible with the field. The out-of-plane magnetic pattern is not sensitive to rotation of the in-plane field. We attribute the observed out-of-plane magnetization component to an out-of-plane magnetic anisotropy, which is a remainder of the [111] magnetic easy axis in bulk $La_{0.67}Sr_{0.33}MnO_3$ single crystal.

DOI: 10.1103/PhysRevB.77.184412 PACS number(s): 68.37.Rt, 75.47.Lx, 75.70.Kw, 75.70.Ak

I. INTRODUCTION

The manganites form a class of magnetic materials with many interesting and yet not fully understood properties. Especially, the hole-doped $La_{1-x}Sr_xMnO_3$ (LSMO) with $x=0.3-0.4$ attracts a lot of attention because of its half metallicity in combination with ferromagnetism up to a relatively high Curie temperature of about 370 K. This combination of properties makes it an interesting model system for application in magnetoelectric devices, as for example tunnel magnetoresistance junctions (TMR junctions).[1–4] However, in practice, the promise of a very high TMR ratio is seldom realized, and junctions cannot be prepared very reproducibly. To solve this problem, much attention is being paid to the material properties of the interface layer of LSMO just underneath the tunnel barrier, which, especially in the case of $SrTiO_3$ (001) (STO) barriers, appears to be strongly affected by the presence of the barrier. Measurements indicate that the LSMO interface is doped with holes from the STO, changing the charge on the Mn ions from on average of about +3.3 to a higher value, which, in turn, changes the properties of this layer from a ferromagnetic metal toward that of an antiferromagnetic insulator.[5–8]

In magnetic tunnel junctions, the tunneling rate depends strongly on the relative orientation of the spins on both sides of the barrier, due to the energy cost of changing the spin of the electron. Information on the structure of the magnetic ordering in the LSMO is therefore crucial for understanding the device performance, since deviations from fully parallel, respectively antiparallel, spin configurations over the complete junction area, required for an optimum TMR, will cause large reductions of this value.

Several factors influence the magnetic ordering and anisotropy in thin LSMO films. It has become clear that a substrate such as STO creates in-plane tensile strain in the LSMO (001) film, causing biaxial anisotropy in the STO [110] and $[1\bar{1}0]$ directions.[9–11] Substrate steps cause a uniaxial magnetic anisotropy axis in the average step edge direction, and there is a competition between these mechanisms if the easy axes do not align. For the samples on low vicinal angle STO, discussed in Ref. 9 it was shown that the strength of the biaxial anisotropy is temperature dependent and starts to dominate at reduced temperatures. For the high vicinal angle STO of Ref. 11, the step-induced uniaxial anisotropy prevails even at low temperatures.

The magnetic domain structure on the (001) surface (in terms of the pseudocubic lattice) of a bulk LSMO single crystal was investigated by spin-polarized scanning electron microscopy.[12] Clear in-plane head-to-head oriented domains were observed in a checkerboard pattern, whereas hardly any out-of-plane magnetization was found. This was thought to result from the (001) cutoff of the bulk domains, oriented in the [111] easy axis direction, where the magnetization lays down to the surface plane.

Recently, photoelectron emission microscopy in combination with x-ray magnetic circular dichroism, a technique that is sensitive to the in-plane orientation of the magnetization, was used on 40 nm thick LSMO on STO, in zero magnetic field. Large stripe domains (approximately 3×30 μm^2) oriented along the crystal steps were found.[13] These domains have blurred contrasts at the domain boundaries. This was suggested to be due to the competition between the uniaxial step anisotropy and the biaxial crystalline anisotropy.

The magnetic force microscopy (MFM) method is a very powerful tool to study magnetic domain structures down to nanometer scale. MFM is mainly sensitive to lateral changes of the out-of-plane component of the force gradient that arise from a long range magnetostatic coupling between the tip and the sample. MFM has been successfully used to detect the strong magnetic contrast on LSMO thin films grown on $LaAlO_3$ (001) (LAO) and $NdGaO_3$ (110) (NGO) substrates.[14–16] The films grown on LAO are in compressive strain in the [100] and [010] directions, forcing the magnetization vector out of plane. A clear mazelike pattern of up and down oriented domains is observed, consistent with a perpendicular anisotropy. Further, the uniaxial compressive strain for LSMO on NGO (110) creates a large out-of-plane magnetization with a stripe domain pattern.

The MFM studies on LSMO thin films grown on STO substrates failed to detect a significant magnetic contrast. The observed MFM pattern is generally described as having a featherlike pattern.[14–16] This is attributed to the magnetization being oriented predominantly in plane, because the film is in tensile strain in the [100] and [010] directions. Thus, there is currently no detailed knowledge about the magnetic domain structure of LSMO on STO (001).

Here, we report on MFM measurements on (001)-oriented epitaxial thin films of LSMO on STO (001) in an in-plane applied magnetic field. In contrast to the literature reports so far, we observe a clear magnetic contrast, using specially selected MFM tips. A magnetic structure in the form of a checkerboard pattern with typical sizes of 0.5–0.75 μm is found. The pattern is not affected by the rotation of the applied magnetic field with respect to the sample orientation and remains essentially unchanged when the field is reduced to zero after the film has been brought to the (almost) saturated state. We argue that the out-of-plane magnetization is a remainder of the [111] magnetic easy axis in bulk LSMO single crystals.

II. EXPERIMENT

Thin LSMO films were deposited on TiO_2-terminated STO (001) substrates[17] with a low vicinal angle ($<0.2°$) by pulsed laser deposition. Film growth was followed *in situ* by reflection high energy electron diffraction (RHEED), and the film thickness was deduced from the RHEED oscillations. The film deposition was performed at a substrate temperature in the range of 750–830 °C in an oxygen pressure of 0.16 mbar. Subsequently, the films were cooled down slowly *in situ* in 1 bar O_2. X-ray diffraction (XRD) confirms the epitaxial growth and the (001) orientation of the overlayer film. Atomically flat terraces with subunit cell rms roughness and parallel steps with a step height equal to the unit lattice cell size of 3.9 Å on the LSMO films were measured with atomic force microscopy. As is well established, LSMO films grow cube on cube on STO (001), and therefore the directions of the LSMO pseudocube crystal structure are those of the STO.

The magnetization was measured with the vibrating sample magnetometer option of the physical property measurement system of Quantum Design.

Two scanning probe microscopes, a Nanoscope IIIa and a DI Dimension 3100, were used for the magnetic force microscopy measurements for zero-field measurements. The similar MFM images obtained with the two microscopes exclude the appearance of artifacts due to the apparatus. For the field dependent measurements, we used the DI Dimension 3100 microscope as it allows the mounting of the yoke. Two types of experimental cantilevers, provided by Nanoworld, were used for the measurements. They consisted of Si tips with a hard magnetic coating of CoCr (coercivity $H_c \approx 20$ kA/m) and a soft magnetic coating of NiCo ($H_c \approx 0.16$ kA/m), respectively.[18] Prior to the measurements, the tips were premagnetized in the surface normal direction, and therefore the tips are predominantly sensitive to the out-of-plane magnetic field component. We performed dynamic MFM measurements in the lift mode. After each topographic line scan, the MFM line scan is performed at a constant predefined distance from the surface where the tip deflection is mainly determined by the magnetic interaction with the stray field of the magnetic film. This enables simultaneous recording of both topographic and MFM images. In the MFM measurements, we have used phase detection, i.e., changes in the cantilever's phase of oscillation relative to the piezo drive. Typically, we used a lift height of 20–30 nm for the MFM images. The lift height was optimized for optimum signal in order to maximize the magnetic signal and to minimize the surface contribution. The MFM measurements were performed at room temperature with and without the application of an in-plane magnetic field at different angles with respect to the step edges on the STO substrate.

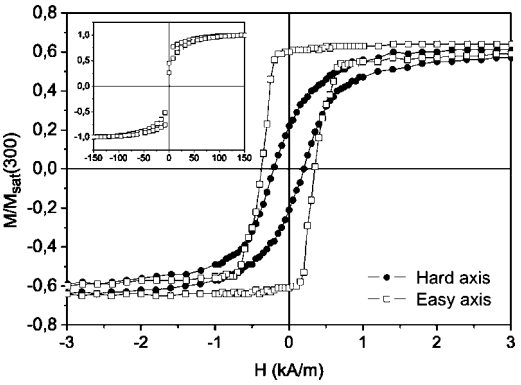

FIG. 1. Magnetic hysteresis loops of 25 nm LSMO film on STO (001), with in-plane applied field along the easy and hard axis of the step-induced uniaxial anisotropy, at room temperature. The inset shows the magnetization measured up to full saturation.

For the MFM measurements in an external magnetic field, we have used a magnetic yoke with an electromagnet, which shows a hysteretic current-field dependence. The remanent magnetization of the yoke is approximately 2.4 kA/m. This is therefore the value of the in-plane field experienced by the sample, when there is no current passing through the coil. The maximum field we have used in our experiments is about 8 kA/m.

III. RESULTS

Figure 1 shows typical room temperature in-plane magnetization hysteresis loops of a 25 nm thick film on STO (001), with the field directed along the easy and hard axes. The low field (few kA/m range) easy axis magnetization is for all film thicknesses only about 65% of the saturation magnetization at this temperature, M_s(300 K). The saturation magnetization is only reached in large in-plane magnetic fields above about 100 kA/m (see inset). The coercive field varies over the range 0.1–0.4 kA/m. Despite the squareness of the easy axis hysteresis loop of the magnetization at low field strengths (Fig. 1), suggesting rapid saturation of the magnetization, a large fraction of the magnetization is not accounted for. This may be present in an out-of-plane magnetization component, or in in-plane components that are not aligned to the field direction yet at moderate field strengths. The low tempera-

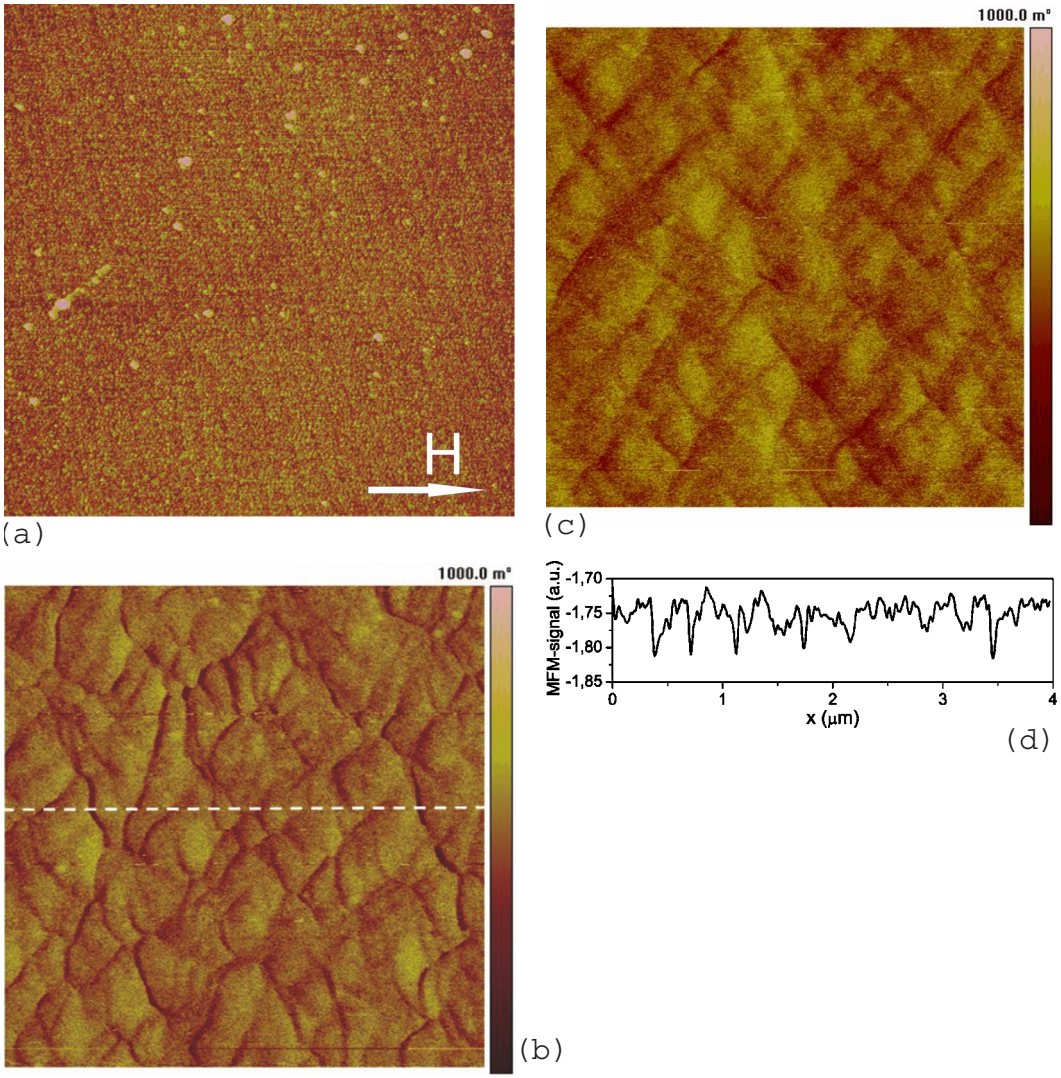

FIG. 2. (Color online) (a) AFM image with a NiCo MFM tip shows the surface steps on a 20 nm $La_{0.67}Sr_{0.33}MnO_3$ film on a $SrTiO_3$ substrate. The scan size is 4×4 μm^2. (b) MFM image of this film taken in 2.4 kA/m in-plane magnetic external field. (c) MFM in 5.6 kA/m magnetic field. (d) MFM line scan along the dashed line in (b). The external field is applied in the direction of the arrow in (a). This is the STO [100] direction.

ture in-plane saturation magnetization corresponds to about 3.5 μ_B/Mn, close to the theoretical maximum value of 3.7 μ_B/Mn, indicating nearly full in-plane alignment of the spins at high fields. For films thicker than about 20 nm, the Curie temperature was found to be at least 350 K.

Two samples were investigated extensively with MFM at room temperature: a 20 nm LSMO film on a 0.14° vicinal angle STO substrate (deduced from the terrace width of about 160 nm) and a 50 nm LSMO film (terrace width 330 nm and vicinal angle of 0.07°). MFM is sensitive to the stray field that comes from the near surface of the film, which, in our case, could well be as large as the film thickness. The coercive field of these films is very low; therefore, the films are always close to the (low field) saturated state due to the remanent field of the yoke.

In order to obtain a good magnetic signal, the choice of the tip is crucial.[19] The CoCr tips gave sufficiently strong magnetic signal to observe the magnetic contrast. However, the magnetic features were highly disturbed during scanning due to the large coercivity and magnetic moment of the tip. Using the soft NiCo tips with a thin coating, the magnetic contrast was not detected, due to the small magnetic moment of these tips. The NiCo tips with the thick coating give the best results for the magnetic images as they satisfy both conditions: a sufficiently large magnetic moment to detect a measurable magnetic signal and a sufficiently small coercive field not to disturb the magnetic features during scanning. The magnetic contrast has been successfully detected with seven different NiCo tips. The range over which the phase typically changed was 0.50°–1°.

Figure 2(a) shows the topography of the LSMO surface of the 20 nm film, obtained with a NiCo MFM tip. The surface steps can clearly be seen, and the step height is approximately 0.4 nm, corresponding to a single unit cell. The steps make an angle of approximately 16° with the [010] direction. Here, and in all MFM plots shown, the sides of the figure are aligned along the [100] and [010] STO crystal directions.

In Fig. 2(b), we show the MFM plot acquired in the same time with the topography plot shown in Fig. 2(a), after cycling the magnet current to the maximum (8 kA/m) and back to zero (2.4 kA/m), with the field applied along the [100] axis. Although the film is in the low field saturated state, clear magnetic contrast is detected with features as small as 20 nm. Darker areas correspond to a negative phase shift caused by an attractive interaction between tip and sample. The field was stepwise increased, and a MFM measurement was made after each step. In Fig. 2(c), we show the MFM image taken in an in-plane magnetic field of 5.6 kA/m. The magnetic structure has changed from the zero-current case, i.e., some features disappeared, the magnetic contrast is reduced, and a more regular pattern, like that of a checkerboard, is formed. The diamond shaped magnetic domains have dimensions of typically 0.5–0.75 μm and thus extend over several terrace widths. We did not find any relation of the pattern orientation with the step edge direction. The sides of the diamonds are roughly in the directions of the [110] and [1$\bar{1}$0] crystal axes. With increasing field, the pattern becomes fader but does not disappear completely, even not at the largest field strengths applied. This is at least partly due to the out-of-plane magnetization rotating into plane, although canting of the tip magnetization with the increased in-plane field cannot be ruled out.

Figure 2(d) shows one of the MFM-signal line scans (thus along the fast scan direction) indicated by the line in Fig. 2(b). The regular pattern of the bright areas and dark lines in Fig. 2(b) is clearly reflected in the corresponding plateaus and sharp dips of the line scan. It is noted that there are no high peaks, which would have shown up as bright lines in Fig. 2(b).

Figure 3 shows three consecutive MFM measurements of approximately the same area of the 50 nm LSMO sample. In this case, the magnetic field is applied along the step edges. Figure 3(a) gives the topographic scan, belonging to the MFM measurement of Fig. 3(b), where the magnetic field is increased in a few steps from 2.4 to 7.6 kA/m while scanning from the bottom to the top of the figure. Also, here the MFM contrast decreases with increasing field strength but does not disappear. The pattern is less regular than in the case of the thin 20 nm film. In Fig. 3(c), we show the MFM image obtained consecutively after Fig. 3(b). The magnetic field is decreased again in a few steps from 7.6 to 2.4 kA/m while scanning from top to bottom. With decreasing field, the contrast increases and the original magnetic pattern is (almost) recovered. At certain steps, where the applied magnetic field has been increased or decreased, one can see "jumps" of the magnetic features marked with circles in Figs. 3(b) and 3(c). The jumps have opposite directions, i.e., in agreement with the variation sense of the applied magnetic field [increasing in Fig. 3(b) and decreasing in Fig. 3(c)]. The jumps are only observed at certain values of the field; otherwise, the magnetic structure is changing gradually. One could argue that the jumps are due to dragging of the magnetic structure in the film by the magnetic tip. However, in that case, one would expect such jumps to occur in more line scans, not only at the line scans corresponding to the field change. A better explanation may be that the magnetic domain structure of the tip changes at specific external field values, changing slightly the lateral sensitivity profile of the tip, in turn causing an apparent shift in the magnetic structure of the film.

The field has also been applied along other directions. The obtained magnetic patterns have similar appearance and do not rotate with the magnetic field direction. Finally, Fig. 3(d) shows the MFM image in the yoke's remanent field of 2.4 kA/m (when no current is passed through the coil of the yoke), scanned immediately after the one shown in Fig. 3(c). The parts of the patterns with less contrast in Figs. 3(b) and 3(c), due to the influence of the magnetic field, now show comparable contrast. In Fig. 3(e), line scans, made along the lines in Fig. 3(b) indicated by the dashed lines, at low, intermediate, and high applied fields (approximately 3.2, 5.4, and 7.2 kA/m) are shown from bottom to top. It shows that the out-of-plane signal, corresponding to the dark features in the MFM images, is reduced with increasing field strength. Some of the boundaries disappear completely whereas others show much less contrast. This is a clear indication for the out-of-plane magnetization rotating into plane in this field range. However, we cannot exclude that part of the reduced signal strength may be due to canting of the tip magnetization with increasing field.

Finally, we draw attention to the observation that the MFM pattern is formed by the dark boundaries, corresponding to attractive tip-sample interaction. There are no bright boundaries, corresponding to repulsive interaction, but rather bright areas within the dark boundaries. MFM measurements on conventional (perpendicular) hard magnetic film using the same NiCo tips show alternating bright and dark domains. This indicates that despite of the low coercivity of the NiCo, the magnetization of the tip is stable during scanning, always pointing in the same direction either toward or away from the surface. However, the domain boundaries of the LSMO film appear always dark indicating that the tip-sample interaction is always attractive in the areas where the magnetization has a large out-of-plane component. Thus, we can conclude that the domain boundaries of the LSMO film are very susceptible to the out-of-plane stray field of the tip and are magnetized during scanning.

IV. DISCUSSION

The MFM measurements of LSMO films on STO reported in literature so far show only little contrast and featherlike patterns, with only gradual changes of the MFM signal. This is generally interpreted as fitting in the model that the magnetization is largely in plane, due to the tensile strain of the film, induced by the STO substrate. This stands in contrast with films on LAO(001) and NGO(110), where there is compressive strain and therefore out-of-plane magnetization, giving rise to the typical mazelike domains[15,16] or bubble magnetic pattern,[14] respectively, stripe domains.[15]

Here, we report on MFM measurements indicating that also for our LSMO films on STO (001) there is a significant out-of-plane magnetization. Furthermore, our results show a significant reduction in signal strength with increasing field, indicating that the out-of-plane magnetization is rotated into the film plane.

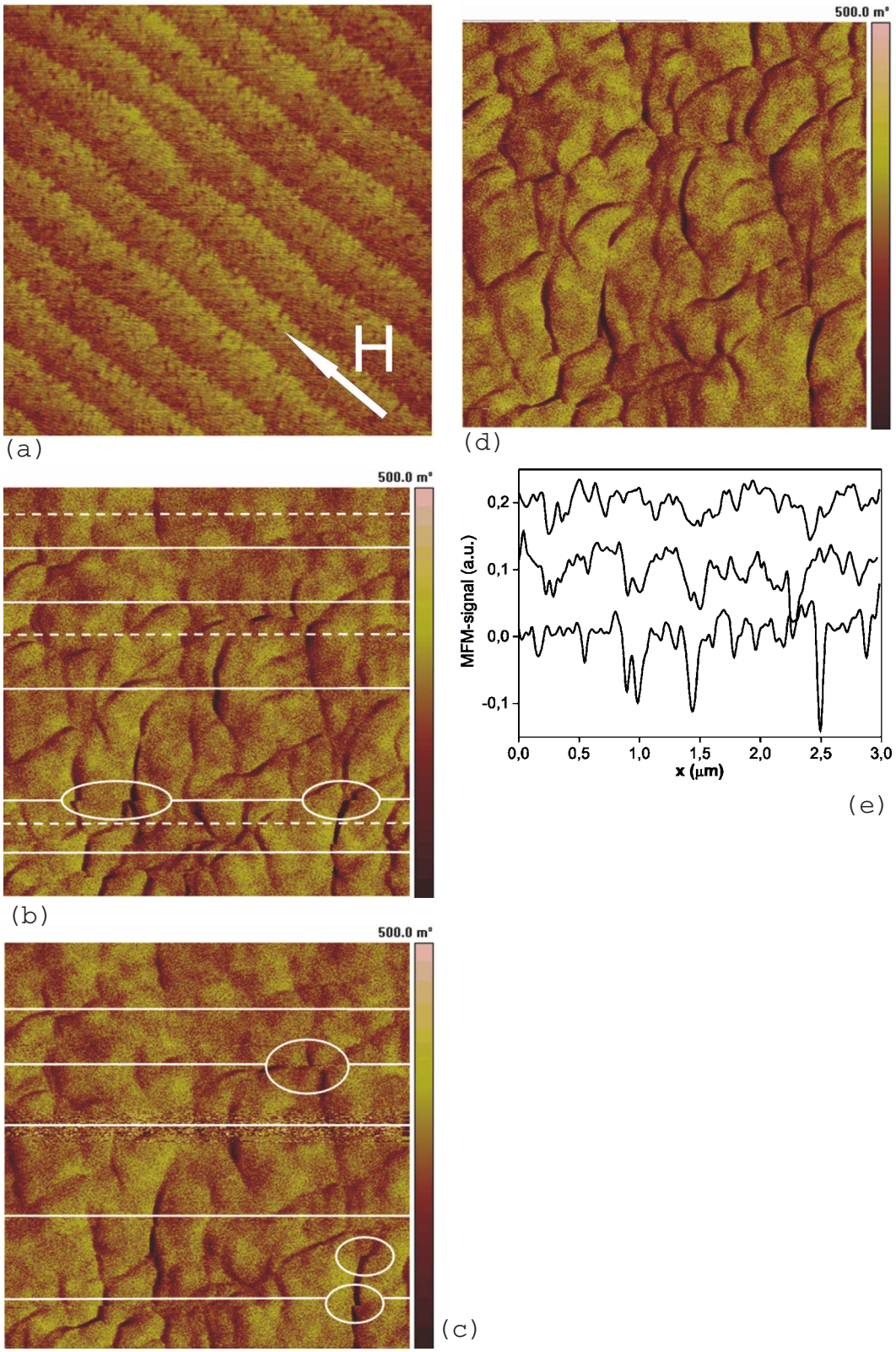

FIG. 3. (Color online) (a) AFM image with a NiCo MFM tip shows the surface steps on a 50 nm $La_{0.67}Sr_{0.33}MnO_3$ film on $SrTiO_3$ substrate. The figures are scanned horizontally and the scan size is 3×3 μm^2. (b) MFM image in an in-plane external field aligned along the step edge direction [the arrow in (a)]. During scanning, the field is increased stepwise from bottom to top from 2.4 to 7.6 kA/m at the position of the solid lines. In the circles, the apparent domain wall jumps when the field is changed from 3.2 to 4.5 kA/m. (c) The MFM image is taken while decreasing the in-plane external magnetic field from top to bottom from 7.6 to 2.4 kA/m. (d) MFM scan acquired immediately after the one presented in (c), in 2.4 kA/m constant field. (e) Line scans at $H=3.2$, 5.4, and 7.6 kA/m, respectively, from bottom to top, corresponding to dashed lines in (b). For clarity, the curves are offset from zero.

The magnetization measurements show that, at the magnetic field strengths H_{MFM} used for the MFM measurements, a large fraction of the magnetization is not accounted for by the in-plane magnetization signal. The remaining fraction may be present in an out-of-plane magnetization component, or in in-plane components that are not yet fully aligned to the field direction at moderate field strengths. This out-of-plane magnetization can be characterized by an out-of-plane anisotropy magnetic field H_{Kperp}, which is of the order of 10 kA/m, above which the MFM contrast vanishes. Further, there is a uniaxial in-plane anisotropy aligning the average in-plane magnetization parallel to the average step direction, as is evidenced by the angle dependent magnetization measurements.[9–11] For the samples discussed here, the corresponding in-plane anisotropy magnetic field $H_{\mathrm{Kpar,lf}}$ is only a few kA/m when in-plane low-field saturation is reached. Only at high field strengths full in-plane alignment is obtained, corresponding to an in-plane anisotropy magnetic field $H_{\mathrm{Kpar,hf}}$ of about 100 kA/m. Thus, the missing fraction of magnetization at zero and low fields is for a small part due to the out-of-plane magnetization component, but for the most part due to incomplete in-plane spin alignment. The latter could be due to a remaining fraction of in-plane 90° or 180° oriented domains, or due to deviations from the average anisotropy direction. The latter is supported by the observation that the substrate steps causing the uniaxial anisotropy are on a microscopic scale neither very straight nor parallel and the local step direction varies over a wide range. The local magnetization direction may follow the local step direction closely. We speculate that this may be the reason why the in-plane magnetization only saturates at the high field strength. This interpretation will be discussed in more detail in a forthcoming paper.

A bulk LSMO single crystal has a [111] magnetic easy axis, due to the rhombohedral distortion of the pseudocubic lattice.[12] A thin LSMO film on STO (001) experiences equal strain in the [100] and [010] directions and has a tetragonal structure, with in-plane lattice constants $a=b=a_{\mathrm{STO}} > a_{\mathrm{LSMO},p}$ and an out-of plane lattice constant $c < a_{\mathrm{LSMO},p}$ (where a_{STO} is the STO lattice constant and $a_{\mathrm{LSMO},p}$ the LSMO pseudocubic lattice constant). One expects in-plane magnetic easy axes oriented along the projections of the {111} directions, which have become equivalent by the biaxial strain. For low vicinal angle STO at low temperature, one indeed finds the in-plane [110] and $[1\bar{1}0]$ easy axes.[9,10] At room temperature[9] or for larger vicinal angle,[11] the associated anisotropy energy is relatively small and the uniaxial step anisotropy dominates. Thus, there is no *a priori* reason to argue that the tensile strain induced by the STO substrate is large enough and that the out-of-plane anisotropy component is reduced to zero. Our MFM measurements clearly indicate that this is not the case.

It is thought that the competition between the remaining out-of-plane anisotropy energy and the magnetostatic energy creates the typical out-of-plane magnetic pattern, minimizing the total magnetic energy. The formation of the checkerboard pattern is ascribed to the biaxial strain for LSMO on STO (001). This is in contrast to the stripe domains observed in LSMO films on NGO (110), exhibiting predominantly uniaxial strain. This is further supported by the observation that in the 20 nm films, experiencing full strain from the substrate, the magnetic pattern is aligned along the maximum strain directions. Thus, the configuration and orientation of the magnetic pattern appear to be imposed by the underlying strain pattern in the film.

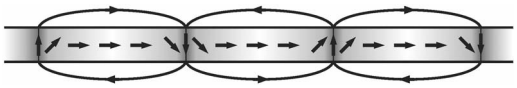

FIG. 4. Schematic drawing of a cross section of the magnetic checkerboard pattern in a LSMO film on STO(001). In the domains, the magnetization is predominantly in plane, and the domains are largely aligned. Due to a finite out of plane anisotropy, the magnetization rotates out of plane at the boundaries. Closed loops are formed to minimize the magnetostatic energy.

Stripe domains are found in films with a weak, spatially uniform out-of-plane anisotropy energy.[20] Experimentally, it is observed that the configuration of stripe domains remains unchanged when the field is rotated, as appears also to be the case for our films with the checkerboard magnetic pattern. Further, it was shown that for a checkerboard pattern, where the magnetization within the squares of the pattern is alternatingly oriented up and down, the magnetostatic energy can be reduced even further. This is somewhat different from the magnetization pattern we observe in our films, where within the squares the magnetization is largely in plane and at the boundaries it is oriented out of plane. However, it seems plausible that the same argument holds here, since the in-plane magnetized areas have minimum demagnetization energy and the perpendicular oriented areas are organized in up and down oriented domains, also minimizing the magnetostatic energy.

In Fig. 4, we have drawn the proposed magnetic structure that explains the observed MFM patterns. In the plane of the film, the magnetization is largely in plane due to the demagnetization and the in-plane tensile strain and it is aligned along the in-plane (local) easy axis. These are the bright areas in the MFM figures. At the boundaries of these domains, the out-of-plane component increases into the $+z$ direction. The external flux line is closed at the opposite boundary, where the out-of-plane magnetization component points in the $-z$ direction. The boundaries are aligned along the high strain directions. Within the domains, the in-plane magnetization aligns along the local in-plane easy axis direction.

We now turn to the difference in the MFM patterns of the 20 and 50 nm samples. The checkerboard pattern is very regular for the thinner 20 nm film, especially at the higher field strengths, whereas for the 50 nm it is fairly irregular. There might be a relation with the distortion of the LSMO lattice in thin films, as was revealed by high resolution transmission electron microscopy[21,22] and synchrotron XRD.[23] It was found that epitaxial LSMO films, grown by PLD on STO and with a film thickness of less than 100 nm, do not show lattice parameter relaxation but undergo a geometric relaxation toward the rhombohedral distortion of its bulk unit cell without the need for dislocations. Hence, one might expect that this strain relaxation is reflected in the orientation

of the spins, being very sensitive to the distortion of the octahedral surrounding of the Mn ions. This may explain the change of the pattern with increasing thickness. The 20 nm film experiences still the full crystalline strain from the substrate, causing the very regular checkerboard pattern, whereas the top part of the 50 nm film has already partly relaxed toward the rhombohedral structure. The magnetic pattern of this film may therefore be due to a mixture of the patterns of a fully strained film and that of a partly relaxed film.

Finally, it is evident that our findings have significant implications for the performance of TMR tunnel devices of LSMO on STO (001). In the magneto-electro investigation of the properties of TMR devices, the electrodes are subjected to a sweeping magnetic field over a fairly small range (a few times the largest electrode coercive field), where, according to the measurements presented here, the out-of-plane component is hardly affected by the applied field. If the tunnel junction area extends over more than a single domain, there will be a large variation in the electron spin alignment, causing a reduction of the TMR. This would explain the relatively poor reproducibility of high TMR devices and why the best TMR results have been reported for very small devices.[1,24] Further, the magnetic domains may be larger at the lower temperatures at which junctions are usually operated, so that the probability that the junction area largely falls within a single domain becomes larger.

V. CONCLUSIONS

In conclusion, we have investigated the out-of-plane magnetization of thin epitaxial LSMO films on STO (001) by magnetic force microscopy, at room temperature. A clear magnetic structure has been observed in this system. The MFM measurement shows a checkerboard pattern, which is interpreted as being due to predominantly in-plane magnetized domains separated by relatively narrow domain boundaries, where the out-of-plane magnetization is largest. The domain boundaries are very susceptible to the out-of-plane stray field of the tip and are magnetized during scanning.

It is argued that the out-of-plane magnetization is due to an out-of-plane magnetic anisotropy, which is a remainder of the [111] easy axis in bulk single crystal LSMO. Although the tensile strain and the demagnetization force the magnetization toward the film plane, the out-of-plane anisotropy appears strong enough to create out-of-plane magnetization. The checkerboard pattern obtained for the 20 nm films is ascribed to the biaxial tensile strain in the film, induced by the STO (001) substrate, in contrast to the stripe domain structure, found in films on substrates creating uniaxial strain as NGO (110). This checkerboard pattern becomes less regular for the 50 nm films due to partial strain relaxation with increasing thickness.

ACKNOWLEDGMENTS

We would like to thank M. Mathews for sample fabrication and J. G. H. Hermsen for the fabrication of the magnet. We acknowledge Nanoworld for providing the NiCo and CoCr MFM cantilevers. This research was supported by NanoNed, a nanotechnology program of the Dutch Ministry of Economic Affairs, and by the ASPRINT European project (NMP-CT-2003-001601).

*Corresponding author. e.p.houwman@utwente.nl
†Present address: CNR-INFM COHERENTIA, Dip. di Scienze Fisiche, Universita' "Federico II" di Napoli, Complesso MonteSantangelo, Via Cinthia, 80126 Napoli, Italy.

[1] M. Bowen, M. Bibes, A. Barthélémy, J. P. Contour, A. Anane, Y. Lemaître, and A. Fert, Appl. Phys. Lett. **82**, 233 (2003).
[2] K. Dorr, J. Phys. D **39**, R125 (2006).
[3] A. M. Haghiri-Gosnet, T. Arnal, R. Soulimane, M. Koubaa, and J. P. Renard, Phys. Status Solidi A **201**, 1392 (2004).
[4] J. H. Park, E. Vescovo, H. J. Kim, C. Kwon, R. Ramesh, and T. Venkatesan, Nature (London) **392**, 794 (1994).
[5] J. W. Freeland, J. J. Kavich, K. E. Gray, L. Ozyuzer, H. Zheng, J. F. Mitchell, M. P. Warusawithana, P. Ryan, X. Zhai, R. H. Kodama, and J. N. Eckstein, arXiv:cond-mat/0611112 (unpublished).
[6] J. J. Kavich, M. P. Warusawithana, J. W. Freeland, P. Ryan, X. Zhai, R. H. Kodama, and J. N. Eckstein, Phys. Rev. B **76**, 014410 (2007).
[7] H. Kumigashira, A. Chikamatsu, R. Hashimoto, M. Oshima, T. Ohnishi, M. Lippmaa, H. Wadati, and A. Fujimori, Appl. Phys. Lett. **88**, 192504 (2006).
[8] H. Kumigashira, R. Hashimoto, A. Chikamatsu, M. Oshima, T. Ohnishi, M. Lippmaa, H. Wadata, A. Fujimori, K. Ono, M. Kawasaki, and H. Koinuma, J. Appl. Phys. **99**, 08S903 (2006).
[9] M. Mathews, F. M. Postma, J. C. Lodder, R. Jansen, G. Rijnders, and D. H. A. Blank, Appl. Phys. Lett. **87**, 242507 (2005).
[10] K. Steenbeck and R. Hiergeist, Appl. Phys. Lett. **75**, 1778 (1999).
[11] Z. H. Wang, G. Cristiani, and H. U. Habermeier, Appl. Phys. Lett. **82**, 3731 (2003).
[12] M. Konoto, T. Kohashi, K. Koike, T. Arima, Y. Kaneko, Y. Tomioka, and Y. Tokura, Appl. Phys. Lett. **84**, 2361 (2004).
[13] T. Taniuchi, H. Kumigashira, M. Oshima, T. Wakita, T. Yokoya, M. Kubota, K. Ono, H. Akinaga, M. Lippmaa, and M. Kawasaki, Appl. Phys. Lett. **89**, 112505 (2006).
[14] R. Desfeux, S. Bailleul, A. Da Costa, W. Prellier, and A. M. Haghiri-Gosnet, Appl. Phys. Lett. **78**, 3681 (2001).
[15] J. Dho, Y. N. Kim, Y. S. Hwang, J. C. Kim, and N. H. Hur, Appl. Phys. Lett. **82**, 1434 (2003).
[16] C. Kwon, M. C. Robson, K. C. Kim, J. Y. Gu, S. E. Lofland, S. M. Bhagat, Z. Trajanovic, M. Rajeswari, T. Venkatesan, and A. R. Kratz, J. Magn. Magn. Mater. **172**, 229 (1997).
[17] G. Koster, B. L. Kropman, G. Rijnders, D. H. A. Blank, and H. Rogalla, Appl. Phys. Lett. **73**, 2920 (1998).
[18] The coating properties were measured on planar substrates.
[19] S. Porthun, L. Abelman, and C. Lodder, J. Magn. Magn. Mater. **182**, 238 (1998).
[20] S. Chikazumi, *Physics of Ferromagnetism* (Oxford University

Press, Oxford, 1997).
[21] R. Lyonnet, J.-L. Maurice, M. J. Hÿtch, D. Michel, and J.-P. Contour, Appl. Surf. Sci. **162**, 245 (2000).
[22] F. Pailloux, R. Lyonnet, J.-L. Maurice, and J. P. Contour, Appl. Surf. Sci. **177**, 263 (2001).
[23] U. Gebhardt, N. V. Kasper, A. Vigliante, P. Wochner, H. Dosch, F. S. Razavi, and H. U. Habermeier, Phys. Rev. Lett. **98**, 096101 (2007).
[24] V. Garcia, M. Bibes, A. Barthélémey, M. Bowen, E. Jacquet, J.-P. Contour, and A. Fert, Phys. Rev. B **69**, 052403 (2004).